DEVELOPMENT OF A REDUCED OXIDATION MODEL FOR HYPERSTOIHIOMETRIC UO_{2+x}

K. Shaheen (MASc Candidate)
Supervisors: B.J. Lewis and W.T. Thompson
Department of Chemistry and Chemical Engineering, Royal Military College of Canada, PO Box 17000, Kingston, Ontario, Canada

Abstract

A numerical treatment was developed for predicting fuel oxidation in uranium-dioxide fuel, using a system of two time-dependent partial differential equations for hyperstoichiometry and temperature. This model was developed as a simplification from a previous mechanistic treatment, against which the current treatment is benchmarked, that also includes equations for hydrogen and steam transport in the fuel-to-sheath gap and fuel cracks. These factors were addressed in the reduced treatment using semi-empirical correlations to increase the model's robustness and computational speed. Further work has involved testing the model against experimental data available from coulometric titration experiments performed at the Chalk River Laboratories.

1. Introduction

For a thermal reactor, such as a CANDU reactor, UO_2 pellets are sheathed within Zircaloy cladding tubes to form fuel elements. Groups of these elements are joined together and sealed with end caps to produce the final fuel bundle. The bundles are inserted into the reactor surrounded by heavy water as a coolant.

Fuel bundles may defect on rare occurrences due to a number of reasons:

- Fretting of fuel cladding can occur due to the possible presence of foreign debris in the coolant circulating around the bundles.
- In some cases, a significant increase in the linear power rating from a low-power rating at high burnup can cause pellet-clad mechanical interaction, and with the presence of reactive fission products such as iodine or cesium, the induced stress can cause Stress Corrosion Cracking (SCC) of the fuel sheathing. It should noted, however, that this defect mechanism has been practically eliminated with the introduction of CANLUB coating.
- Cracking can also occur near the end cap welds through increased stress due to hydrogen diffusion to these areas of low temperature. This is known as Delayed Hydrogen Cracking (DHC).
- Alternately, in very rare occurrences, end caps may crack or even break off as a result of faulty fabrication or welding and secondary hydriding processes.

Such defects are extremely rare; less than 0.1% of CANDU fuel bundles develop defects [1]. However, they can negatively impact fuel performance when they do occur. Defects in the fuel cladding and end caps expose the fuel pellets to the surrounding environment, allowing fuel to be lost into the coolant stream around the fuel bundle. This situation also allows the coolant to seep through the cladding and to interact with the fuel pellet directly. In such a case, the exposure to the high temperature UO_2 causes the heavy water coolant to flash to vapour.

The heavy water vapour can react with the UO_2 pellets to form hyperstoichiometric UO_{2+x}. The single-phase UO_{2+x} can affect fuel behaviour. The fuel thermal conductivity decreases with hyperstoichiometry [2], causing the centerline fuel temperature to rise. The incipient melting temperature of hyperstoichiometric fuel is also reduced. Determining the extent of fuel oxidation, and its subsequent effects on the fuel behaviour, is therefore required.

2. Background

A finite-element numerical model of fuel oxidation behaviour has been previously produced [3]. This model is used as the starting point for development of the current work. The mechanistic treatment addresses four primary mechanisms for the overal fuel oxidation behaviour:

(i) Hyperstoichiometry (x): Vapour can react with solid fuel, producing hyperstoichiometric UO_{2+x}, as a result of interstitial oxygen diffusion.
(ii) Temperature: The temperature (T) in the fuel is affected by the changing thermal conductivity in hyperstoichiometric fuel.
(iii) H_2/H_2O transport in the gap: The hydrogen mole fraction (q) in the fuel-to-clad gap is determined by the axial transport and reaction kinetics of steam/hydrogen with the fuel and cladding.
(iv) H_2/H_2O transport in the fuel: The hydrogen mole fraction q is further determined by the radial transport and reaction kinetics of steam/hydrogen within the fuel cracks of the pellet.

In the current treatment, reference is made to steam (H_2O) and hydrogen gas (H_2); however, in an equivalent way, this discussion also pertains to heavy water vapour (D_2O) and deuterium gas (D_2).

The above processes are all interrelated: the thermal conductivity, which determines the temperature, is a function of the fuel temperature and extent of hyperstoichiometry. The fuel oxidation reaction potential is in turn determined by the hydrogen mole fraction in the gap and the cracks and the fuel temperature. Any attempt to model such a system will produce highly non-linear equations. In this case, a system of four coupled partial differential equations, one for each of the respective mechanisms listed above, is set up as shown [3]:

(i): $$\frac{\partial x}{\partial t}=\frac{\partial}{\partial z}\left(D\frac{\partial x}{\partial z}\right)+\frac{1}{r}\frac{\partial}{\partial r}\left[rD\left(\frac{\partial x}{\partial r}+x\frac{Q}{RT^2}\frac{\partial T}{\partial r}\right)\right]+\sigma_f R_f^{react}$$ **Equation 2.1**

(ii): $$\rho_s C_p\frac{\partial T}{\partial t}=\frac{\partial}{\partial z}\left(k\frac{\partial T}{\partial z}+\frac{1}{r}\frac{\partial}{\partial r}\left(rk\frac{\partial T}{\partial r}\right)+\frac{P_{lin}}{\pi a_p^2}\left[\frac{(\kappa a_p)}{2I_1(\kappa a_p)}\right]I_o(\kappa r)\right)$$ **Equation 2.2**

(iii): $$c_g\frac{dq}{dt}=\frac{\partial}{\partial z}\left(c_g D_g\frac{\partial q}{\partial z}\right)-\frac{\partial}{\partial z}\left(qc_g u\right)+\sigma_g\left(R_{clad,Zry}^{ox,post}-R_{clad,Zry}^{H_2,post}+R_{fuel}\right)$$ **Equation 2.3**

(iv): $$\varepsilon c_g\frac{\partial q}{\partial t}=\frac{\varepsilon}{\tau^2 r}\left[\frac{\partial}{\partial r}\left(rc_g D_g\frac{\partial q}{\partial r}\right)\right]+\sigma_f R_f^{react}$$ **Equation 2.4**

The system is for a two-dimensional model in the fuel with cylindrical coordinates in the radial (*r*) and axial (*z*) direction as depicted in Figure 1, and time (*t*). The parameters of the model are detailed in Table 1.

Table 1: Parameters of mechanistic model

Expression	**Description**
D	Solid state diffusion coefficient of interstitial oxygen
Q	Effective heat of transport (Soret effect)
R	Ideal gas constant
σ_f	Fuel surface-to-volume ratio
R_f^{react}	Fuel oxidation/reduction reaction rate term
ρ_s	Fuel density
C_p	Heat capacity in the fuel
k	Thermal conductivity in the fuel
P_{lin}	Linear power rating
a_p	Pellet radius
$\left[\frac{(\kappa a_p)}{2I_1(\kappa a_p)}\right]I_o(\kappa r)$	Neutron flux depression effect in the pellet
c_g	Total molar concentration of gas in the gap
$c_g D_g$	Gaseous diffusion term
u	Bulk-flow molar velocity in the gap due to pressure differential
σ_g	Ratio of sheath surface to gap volume
$R_{clad,Zry}^{ox,post}$	Sheath corrosion reaction rate term
$R_{clad,Zry}^{H_2,post}$	Sheath hydrogen pickup reaction term
R_{fuel}	Fuel-to-gap hydrogen flux
ε	Volume of cracks to total fuel volume ratio
τ	Tortuosity factor in the fuel cracks

This system was solved by the finite-element method using the COMSOL Multiphysics software package. The results were validated using experimental data provided by the Chalk River Laboratories (CRL) of Atomic Energy of Canada Limited (AECL).

3. Reduced model development

The reduced model aims to determine fuel hyperstoichiometry and temperature in a manner consistent with the mechanistic approach, while reducing the numerical complexity of the system in order to enhance the model's robustness and efficiency.

3.1 Temperature equation

To maintain consistency, the temperature equation in the reduced model is the same as that in the mechanistic:

$$\rho_s C_p \frac{\partial T}{\partial t} = \frac{\partial}{\partial z}\left(k \frac{\partial T}{\partial z} + \frac{1}{r}\frac{\partial}{\partial r}\left(rk \frac{\partial T}{\partial r} \right) + \frac{P_{lin}}{\pi a_p^2}\left[\frac{(\kappa a_p)}{2I_1(\kappa a_p)} \right] I_o(\kappa r) \right) \qquad \textbf{Equation 3.1}$$

3.2 Hyperstoichiometry equation

Observations of the mechanistic model indicate that the fuel oxidation reaction takes place primarily under the defect in a given rod, as shown in the two-dimensional representation of the sample case in Figure 1. It should be noted that this case represents a single, mid-rod defect, and thus its axial dimension is half the size of a typical rod, with symmetry assumed in the other half of the rod.

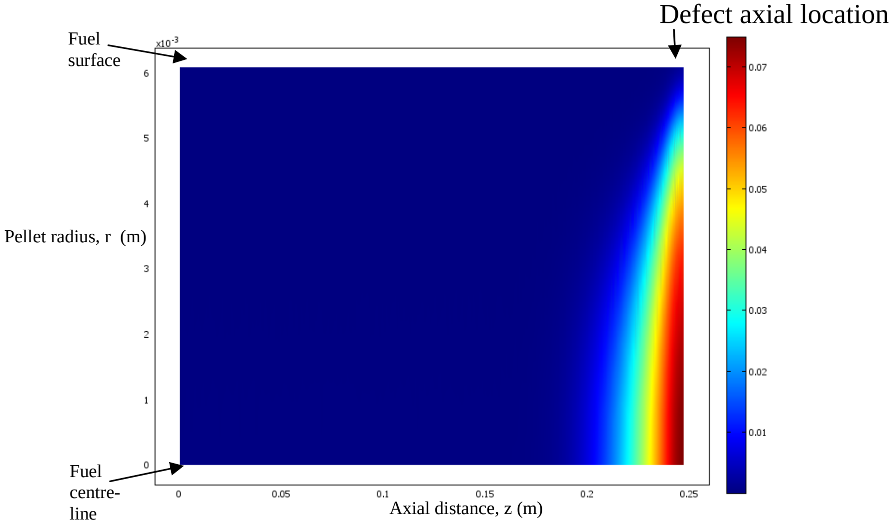

Figure 1 Stoichiometry deviation, *x*, under a 10 mm defect as compared to general element body at 25 kW m^{-1}.

The scale on the right refers to the extent of hyperstoichiometry *x* in the UO_{2+x}. It can be seen that excess oxygen exists almost entirely under the defect site (i.e., at the axial location of the defect). Away from the defect site, an increase in the hydrogen mole fraction inhibits the fuel oxidation potential. Thus, any hyperstoichiometry away from defect sites will be primarily due to solid-state oxygen diffusion through the fuel element.

Based on this result, it is postulated that the reactions taking place under defects serve as an ‘engine’ for the oxidation of the non-defected regions. Hence the equations can be simplified so that only radial diffusion must be considered at the defect location. Away from these locations, semi-empirical correlations can be used to capture the effects of the axial transport of oxygen. A conceptual model of this approach is shown in Figure 2.

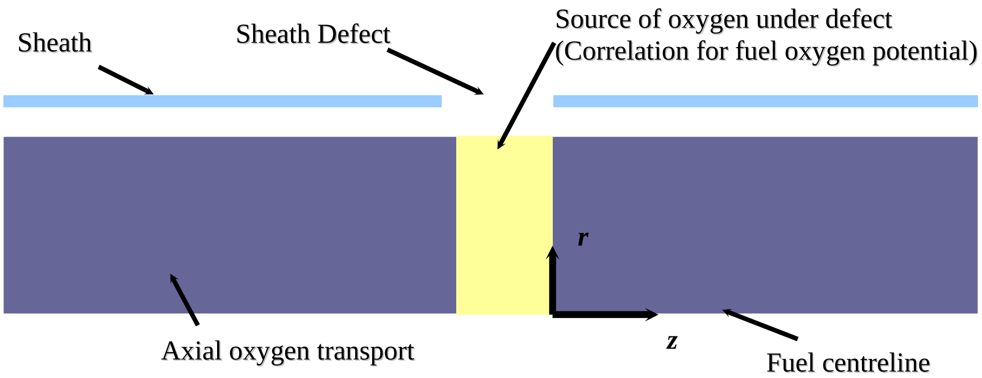

Figure 2 Modeling of fuel oxidation under the defect site for the reduced model.

The hyperstoichiometry equation at the defect location is now given by:

$$\frac{\partial x}{\partial t} = \frac{1}{r}\frac{\partial}{\partial r}\left[rD\left(\frac{\partial x}{\partial r} + x\frac{Q}{RT^2}\frac{\partial T}{\partial r}\right)\right] + \sigma_f R_f^{react} \qquad \textbf{Equation 3.2}$$

This differs from the mechanistic equation in that the axial diffusion term has been removed. Thus, this equation is now solved in one dimension, while remaining coupled to the two-dimensional temperature equation. COMSOL Multiphysics permits a one-dimensional equation to be solved on a two-dimensional geometry as shown in Figure 3:

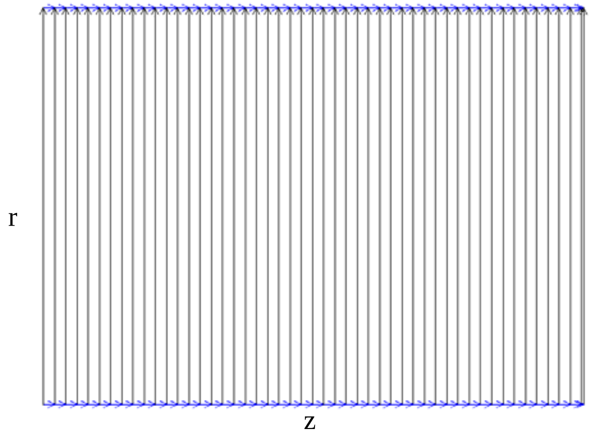

Figure 3 Geometry for the one-dimenstional fuel oxidation model and two-dimensional heat conduction model.

Hence, the temperature equation is solved in the axial and radial directions throughout the two-dimensional region. On the other hand, the hyperstoichiometry equation is solved only in the radial direction along the vertical lines, and the *x* values are linearly interpolated between these solutions. Along each of these lines, COMSOL solves the hyperstoichiometry equation using a "weak boundary mode" [4].

For the effect of radial diffusion of interstitial oxygen, both normal solid-state diffusion (due to a concentration gradient), and Soret diffusion (due to a thermal gradient), are considered. The surface-exchange model for the reaction rate of fuel oxidation or reduction, R_f^{react}, is given by [3]:

$$R_f^{ox} = c_U \alpha \sqrt{(1-q)p_t}\left(x_e - x\right), \quad \text{for } x < x_e$$

Equation 3.3

$$R_f^{red} = c_U \alpha \sqrt{q p_t}\left(x_e - x\right), \qquad \text{for } x > x_e$$

where c_U is the molar density of uranium in UO_2, p_t is the total pressure of the system, α is the surface-exchange coefficient of oxygen, and x_e is the equilibrium stoichiometry deviation. This latter quantity is determined by equating the oxygen partial pressure in the fuel to the oxygen potential in the surrounding hydrogen/steam (H_2/H_2O) environment. The fuel oxygen potential is determined, as in the mechanistic treatment, from the uranium-oxygen phase diagram, shown in Figure 4 [3]:

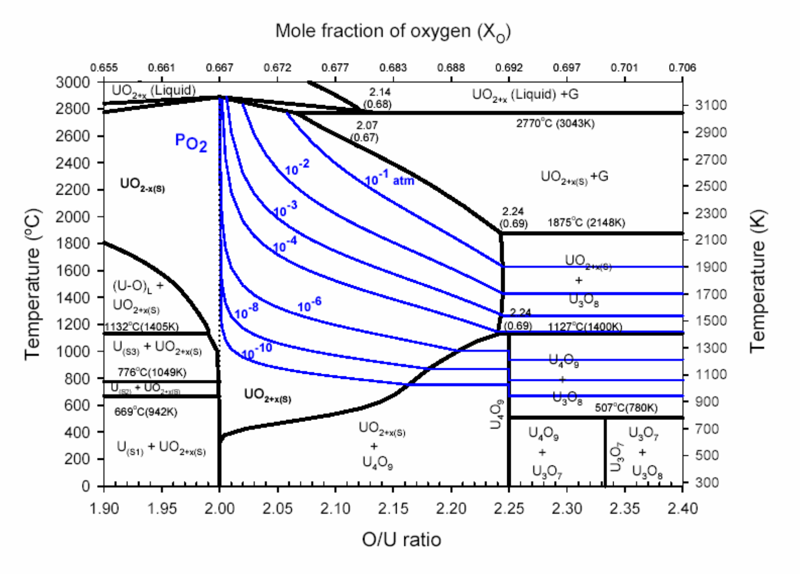

Figure 4 U-O phase diagram with oxygen partial pressure lines.

With H_2O as the source of excess oxygen, the oxygen potential can be related to the H_2/H_2O partial pressure ratio. As such, x_e can be evaluated as a function of the hydrogen mole fraction q and T [3]. Thus, the hydrogen mole fraction must be known in order to solve the fuel oxidation equation. However, it is no longer solved using the two partial differential equations given in the mechanistic model (Equation 2.3 and Equation 2.4). Instead, semi-empirical correlations have been developed for q at and away from the defect locations, given as q_{def} and q_{axial}, respectively.

3.3 Determining q_{def}

The hydrogen mole fraction is required in order for the stoichiometry deviation under the defect to be accurately predicted. By studying test cases with the mechanistic model under a variety of circumstances, it was found that q_{def} is primarily dependant on the linear power rating, as well as the maximum defect size.

Based on this approach, the mechanistic model was run for a number of cases covering the range of power ratings and defect sizes expected in fuel elements under typical operating conditions. The reduced model was solved for all of these cases, with q_{def} tuned to match the stoichiometry deviation and temperature results of the mechanistic model at the various defect locations. The q_{def} values obtained via this approach for the reduced model are shown in Figure 5.

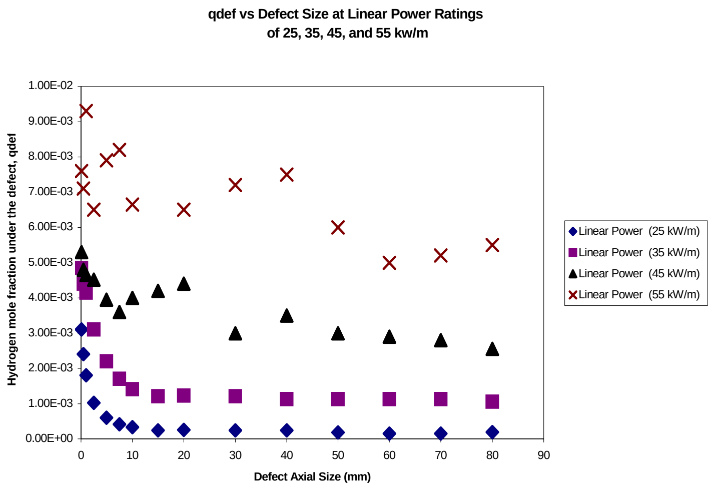

Figure 5 q_{def} values used in the reduced model that reproduce the results of the mechanistic model.

While the graph suggests a trend in the data, there does not appear to be a simple function capable of reproducing the q_{def} values to the required accuracy. Current work is therefore focusing on the use of Legendre polynomials to improve the accuracy of the correlation.

3.4 Determining q_{axial}

As shown in Figure 1, the stoichoimetry deviation decreases with the increased distance from the defect location. This observation is associated with the production and presence of hydrogen away from the defect site. Based on this result, in a similar manner to that outlined in Section 3.3, the q values required to match the hyperstoichiometry and temperature of the mechanistic model at different distances away from the defect were found. Sample results are shown in Figure 6.

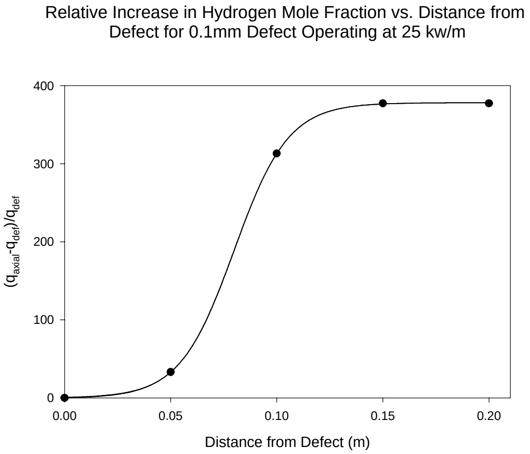

Figure 6 Developing a correlation for q_{axial}.

The curve in the above graph is a sigmoid function predicting the relative ratio $\frac{q_{axial}-q_{def}}{q_{def}}$ with respect to distance. This function is given by:

$$\frac{q_{axial}-q_{def}}{q_{def}} = \frac{a}{1+e^{-\left(\frac{dist-b}{c}\right)}} + d \qquad \textbf{Equation 3.4}$$

where *dist* is the distance away from the defect location, a = 378.8247, b = 0.0128, c = 0.0798, and d = -0.7157. For a range of power ratings from 25 kw m^{-1} to 55 kw m^{-1}, and defect sizes from 0.1 mm to 80 mm, sigmoid functions of the same form were developed. A linear interpolation for interim power ratings and defect sizes allowed for the determination of q_{axial} in all cases explored.

3.5 Boundary conditions for the fuel oxidation model

Reflexive boundary conditions at r = 0 for both T and x are needed to represent the axial symmetry about the fuel centerline. The two axial ends of the rod have no reactions occurring due to the presence of the end caps, and are also considered to be thermally insulated. As such, reflexive boundary conditions are set for T along these boundaries as well. The fuel surface temperature was determined independently in the mechanistic model, and is typically in the range of 650 to 750 K. Within this temperature range, the phase diagram in Figure 4 indicates that no significant hyperstoichiometry is possible, and so x is set equal to x_e. The initial condition (at t = 0) assumes that the fuel is stoichiometric (x = 0) and the temperature through the fuel body is equal to the fuel surface temperature.

Comment [BJ1]: I though x was a 1-D model in Eq. 3.2, therefore there is no reflexive condition required at the ends of the rod?

4. Results

The model was benchmarked against the mechanistic model, and then tested against available experimental data.

4.1 Comparison to mechanistic model

The first test of the correlations for q_{def} and q_{axial} was performed by comparing the results of the reduced model to those of the mechanistic one. This was performed for the full range of power ratings and defect sizes, and produced the expected agreement. A sample comparison of hyperstoichiometry and temperature for a rod operating at 35 kw m^{-1} with a 5 mm defect located at z = 0.247 m is shown in Figure 7. As is the case in the previous example in Figure 1, the rod shown in Figure 7 is half the length of a typical rod, with symmetry assumed in the other half.

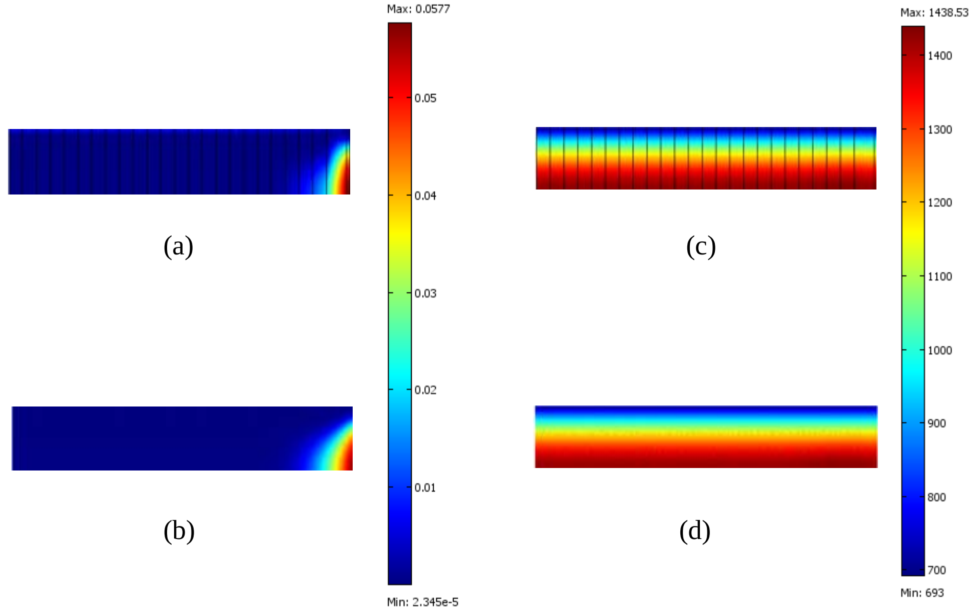

Figure 7 Comparison of x for the reduced model (a) and mechanistic model (b), and T (K) for the reduced model (c) and mechanistic model (d).

A more precise comparison is shown by comparing the axial profiles at various radial locations in Figure 8.

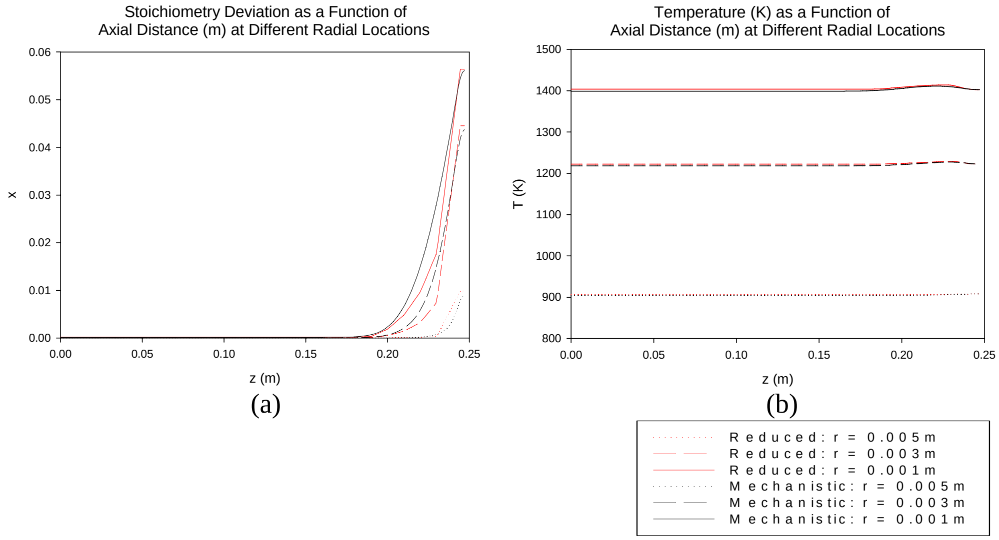

(a)

(b)

Figure 8 Axial profiles of hyperstoichiometry (a) and temperature (b) at various radial locations.

4.2 Comparison to experimental data

Experimental measurements of stoichiometry deviation were performed on nine defective fuel elements from commercial power reactors, and one from the NRU experimental reactor at the Chalk River Laboratories (CRL) [5]. These measurements were performed using a coulometric titration method, where the sample is exposed to a gas stream of known oxygen potential, after which the change in the gas oxygen potential is measured, allowing the quantity of oxygen in the sample to be deduced [5]. The provided data are used to validate the current model [6]. A sample comparison of the experimental data with both the reduced model and the mechanistic model is shown in Figure 9.

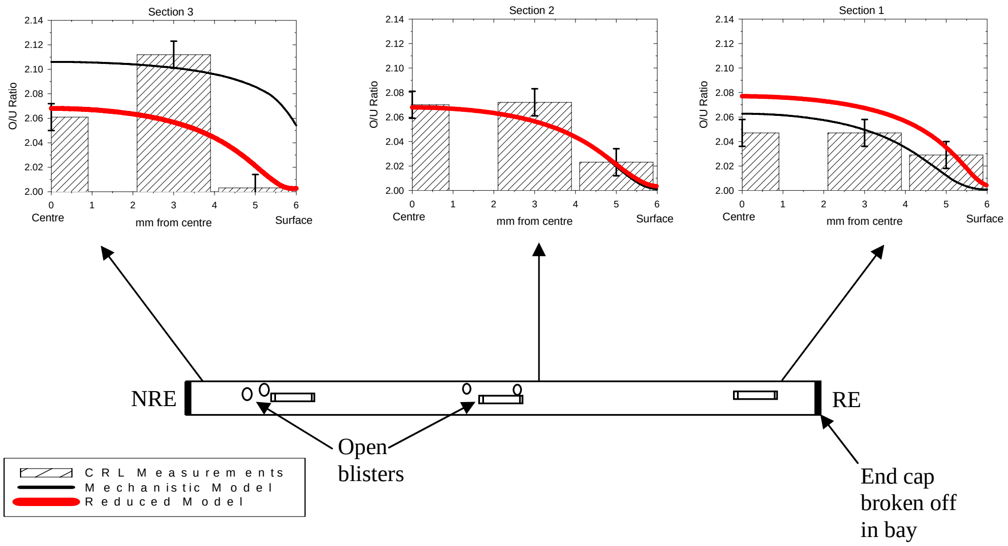

Figure 9 Comparison of hyperstoichiometry results from reduced model and mechanistic model to measurements from CRL for an element at 43 kw m^{-1} with three axial defects.

5. Discussion

The correlations for the reduced model demonstrate reasonable agreement with the mechanistic model across the explored range of power ratings and defect sizes. This result indicates that the conceptual approach of the reduced model, as well as the method of its implementation, are sound. The reduced model also demonstrates reasonable agreement with the experimental data (as shown in Figure 9); however, for some cases, the reduced model underpredicts the amount of fuel oxidation. Two probable causes for these discrepancies are being explored:

- The sigmoid functions for q_{axial} were developed using single defect cases, as in Figure 1, whereas the rods studied by CRL are all multiple defect cases. It has been observed that in the presence of multiple defects, more oxygen is transported into the regions between defect locations. Based on this observation, a new correlation for q_{axial} is currently being developed for multiple-defect cases.

- In some cases, the rod may have a variable power and defect history. While this is simulated in the reduced model, it may be necessary to include a term for the time dependence of $q_{def,}$ to better represent this behaviour.

These effects are currently being explored in order to improve the model representation.

6. Conclusion

A reduced fuel oxidation model has been developed. The model results are in reasonable agreement with a previous mechanistic treatment, and show reasonable agreement with the available experimental data. Further work is focusing on improving the correlations for the hydrogen mole fraction at the defect location, as well as the correlations for the axial variation in the hydrogen mole fraction along the fuel-to-sheath gap.

7. Acknowledgements

The author would like to acknowledge the support of AECL-CRL (Dr. Z. He and Dr. R. Verrall) for their experimental measurements of the O/U ratio in commercial defective fuel. This work was supported by a Collaborative Research and Development Grant with the Natural Sciences and Engineering Research Council of Canada (NSERC) and the CANDU Owner's Group (COG). Additional support was provided through an ATEC Fellowship. The author is grateful for the continued guidance and support of Dr. B.J. Lewis and Dr. W.T. Thompson.

8. References

[1] Lewis B.J., *Nuclear Fuel Engineering*, Royal Military College of Canada, Course Notes NE 533, pp.'7-1'.
[2] Lucuta P.G., Matzke Hj., Hastings I.J., "A pragmatic approach to modeling thermal conductivity of irradiated UO_2 fuel: review and recommendations", *Journal of Nuclear Materials*, Iss. 232, 1996, pp. 166-180
[3] Higgs J.D., "Modeling oxidation behaviour in operating defective nuclear reactor fuel elements", PhD Thesis, Royal Military College of Canada, 2006.
[4] "Theoretical Background", *COMSOL Modeling Guide*, COMSOL Inc, Burlingston, MA, USA, 2006.
[5] Verrall R.A., He Z., and Mouris J., "Characterization of fuel oxidation in rods with clad-holes", *Journal of Nuclear Materials*, Iss. 344, 2005, pp. 240-245.
[6] Higgs J.D., Lewis B.J., Thompson W.T., and He Z., "A conceptual model for the fuel oxidation of defective fuel", *Journal of Nuclear Materials*, in press.